Progress In Electromagnetics Research B, Vol. 16, 57–84, 2009

ELECTROMAGNETIC SOURCE EQUIVALENCE AND EXTENSION OF THE COMPLEX IMAGE METHOD FOR GEOPHYSICAL APPLICATIONS

A. Pulkkinen †

University of Maryland, Baltimore County
Maryland, USA

A. Viljanen, R. Pirjola, and L. Häkkinen

Finnish Meteorological Institute
Helsinki, Finland

Abstract—In this work, source equivalence and computation of the reflected (induced) electromagnetic field in geophysical situations are studied. It is shown that the application of Huygens' principle allows for full generalization of Fukushima's equivalence theorem that applies only for magnetic field. The source equivalence is revisited for a vertical line current element, and it is shown that the equivalent charge required to replace the original source by a planar equivalent source together with the surface charge associated with the reflected field generates a purely vertical total electric field on the ground. Consequently, if the magnetic field and horizontal components of the total electric field on the ground are of interest, only equivalent currents need to be considered. The classical Complex Image Method (CIM) is derived from the exact image theory for planar impedance surfaces. The classical CIM is extended by considering a divergence-free source current that may have components also perpendicular to the ground plane. The extension is seen to generate a complex image charge not present in the classical CIM. Further, a generalized application of the extended CIM to geophysical situations having divergence-free volume source currents is introduced. The application involves decomposition of the source into linear current elements and rotations, translations and reflections of the electromagnetic field expressions associated with each element. The validity of the new approach is verified for an

Corresponding author: A. Pulkkinen (antti.a.pulkkinen@nasa.gov).
† Also with NASA Goddard Space Flight Center, Maryland, USA.

example of external current system and ground model setup by means of comparisons to results obtained from exact formulation by [18].

1. INTRODUCTION

The concept of image sources used to replace physical structures has been known for a long time and is especially well-known in electrostatics where it was already applied by Lord Kelvin [1, p. 52–85]. Although it seems that the non-static generalization was first developed in acoustics [2] (Taraldsen points out that "the method has a tendency of being rediscovered"), the approximate formulation of the concept to temporally varying electromagnetic fields resulting in discrete images at complex depths was introduced to quasi-static geophysical settings by [3, 4] (see also [5]). The most general form of the image theory involving continuous distribution of images leading to exact representation of the fields reflected from planar structures was developed in a series of Exact Image Theory (EIT) papers by [6–8] (see also [9]).

The central idea in the application of the images to electromagnetic induction problems is to replace the medium giving rise to reflected fields by an electromagnetic source that is hoped to make the problem mathematically more tractable or the physical interpretation of the problem more appealing. The standard approach used to determine the source involves finding some convenient representation for the field reflection coefficient mapping the incoming waves to reflected/outgoing waves; the new representation of the reflection coefficient is then used to interpret the reflected field being a certain distribution of electromagnetic sources, i.e., image sources, within the medium. The great appeal of the approximate image method for quasi-static geophysical applications, put forward by [3, 4], is that the usage of only the first a few terms of the series expansion of the reflection coefficient leads to a discrete image source, the depth of the source being a function of the properties of the medium. The discrete image implies that once the incident electromagnetic field generated by the original source is known, the reflected field can be obtained simply by replacing the height of the source by the (complex) depth of the image. Using this approach one avoids analytically usually non-tractable and numerically very time-consuming integration of the equations associated with the electromagnetic induction in the ground (for various numerical techniques as applied to different electromagnetic problems, see e.g. [10–13]). With simplified source geometries this so-called Complex Image Method (CIM) leads to a great advantage in time-critical

applications such as space weather forecasts. CIM has been used in this context in a number of papers investigating the Geomagnetically Induced Current (GIC) phenomenon (e.g., [14, 15]).

The classical CIM as formulated by [16] is able to handle only divergence-free source currents confined to a plane. [17] extended the classical CIM to situations having more general volume currents by means of source equivalence to be discussed in detail later in the paper. Importantly, the extension by [17] allows for the treatment of geomagnetic induction at high-latitudes where the field-aligned currents can be assumed to be perpendicular to the ionospheric plane, i.e., the currents are vertical. The main motivation for the present work comes from the need to model electromagnetic induction (and GIC) at lower latitudes where the verticality of the field-aligned currents cannot be assumed. The generalization of CIM to situations having non-vertical field-aligned currents, studied earlier in non-CIM context by [18], necessitates both better understanding of the source equivalence between three-dimensional volume source currents and two-dimensional surface currents and CIM's general relation to volume currents.

It will be shown in this work that the source equivalence can be understood on a general level by a straightforward application of Huygens' principle. Huygens' principle enables a full generalization of the well-known Fukushima's source equivalence theorem [19], which is applicable only for the magnetic field, for both electric and magnetic fields and for arbitrary surface geometries. It will be seen that, in principle, the general source equivalence that considers the total, instead of only incident, electromagnetic field enables the usage of the classical CIM with complicated volume currents. However, it will be shown by deriving the classical and extended CIM from EIT that the mapping of volume source currents into equivalent sources is, in fact, not necessary; extended CIM can be used to provide the total electromagnetic field directly from the known structure of the source and expressions for the incident field.

Extended CIM was derived from EIT for a homogeneous ground by [20]. However, in geophysical situations a homogeneous ground is often not a very good approximation, and the usage of a layered ground enables a more accurate inclusion of the wide frequency band associated with the geomagnetic induction (e.g., [21]). Thus, it is of interest to formulate CIM in a way that allows for the usage of layered ground structures, as in the works by [22] and [17]. To address this need, CIM is derived here from EIT expressions formulated for planar impedance surfaces associated with arbitrary layered conductivity profiles. The derivation ultimately results in a generalization of the

classical CIM formulation by [16] and of the extended CIM by [17] by inclusion of volume currents having arbitrary orientation with respect to the ionospheric plane.

The practical application of CIM is greatly simplified when the source is decomposed into geometrically simple elements (such as loops used by [17]). Here CIM is applied by means of linear element representation of a divergence-free volume current. The elements can have arbitrary orientations, and the representation thus requires transformations between different coordinate systems. The operators needed to carry out the transformations are also presented. The generalized element representation combined with the derived extended CIM expressions will allow a computationally efficient consideration of the electromagnetic induction in a layered ground, for example, at latitudes where the verticality of the field-aligned currents cannot be assumed.

In summary, the following new results will be derived. 1) The general source equivalence will be applied to geophysical situations to show that the equivalent charge together with the surface charge required by the current continuity do not create a horizontal electric field on the ground. This will validate the use of only equivalent currents in the extended CIM by [17]. 2) CIM will be derived from EIT, and the classical CIM will be extended to situations where the source current can have any orientation. This will generalize [17], where a combination of horizontal and purely vertical currents was studied. 3) A new practical technique for application of the generalized CIM will be introduced.

2. EQUIVALENT SURFACE REPRESENTATION OF VOLUME CURRENTS

In this section, results that enable the mapping of three-dimensional volume source currents into equivalent two-dimensional surface sources are presented. First, fundamentals of the mapping by means of Huygens' principle are reviewed. Then the formulation is applied to the fields associated with planar surfaces, and the derivation of the equivalent sources for a vertical line current element is revisited. Also, the source equivalence with respect to incident versus total electromagnetic field is discussed.

2.1. Source Equivalence Based on Huygens' Principle

[23] (see also [24, Chapter 6]) carried out an elegant derivation of the surface equivalent electromagnetic sources by means of Huygens'

principle. In short, [23] defined a step function as

$$P(\mathbf{r}) = 1 \quad \mathbf{r} \in V, \qquad P(\mathbf{r}) = 0 \quad \mathbf{r} \notin V \tag{1}$$

and multiplied Maxwell's equations by $P(\mathbf{r})$ to obtain truncated Maxwell's equations

$$\nabla \times \mathbf{E}_V + \partial_t \mathbf{B}_V = \nabla P \times \mathbf{E} \tag{2}$$
$$\nabla \times \mathbf{H}_V - \partial_t \mathbf{D}_V = \mathbf{J}_V + \nabla P \times \mathbf{H} \tag{3}$$
$$\nabla \cdot \mathbf{B}_V = \nabla P \cdot \mathbf{B} \tag{4}$$
$$\nabla \cdot \mathbf{D}_V = \rho_V + \nabla P \cdot \mathbf{D} \tag{5}$$

where a notation

$$\mathbf{F}_V = P\mathbf{F} \tag{6}$$

is used. In Eqs. (2)–(5) $\mathbf{E}$ and $\mathbf{H}$ denote the electric and magnetic fields, $\mathbf{D}$ and $\mathbf{B}$ the electric and magnetic flux densities and $\mathbf{J}$ and ρ the electric currents and charges, respectively. Following Huygens' principle, Eqs. (2)–(5) describe the fields in V generated by sources on the right-hand side of the equations. The truncation of the sources outside V is seen to give rise to additional sources

$$\mathbf{J}_{mH} = -\nabla P \times \mathbf{E} \tag{7}$$
$$\mathbf{J}_H = \nabla P \times \mathbf{H} \tag{8}$$
$$\rho_{mH} = \nabla P \cdot \mathbf{B} \tag{9}$$
$$\rho_H = \nabla P \cdot \mathbf{D} \tag{10}$$

where subscript m denotes magnetic currents and charges. Since

$$\nabla P = \delta(\mathbf{s})\mathbf{n} \tag{11}$$

where δ is the Dirac delta function; $\mathbf{s} \in S$ and $\mathbf{n}$ is the normal unit vector of the surface; the sources in Eqs. (7)–(10) are confined to the surface S of volume V (see Fig. 1). These new sources are called Huygens' equivalent sources, and they facilitate the mapping of the volume currents outside V to equivalent sources on the surface S. It is noted that Fukushima's equivalence theorem [19] well-known to geophysicists considered only the source (8).

By taking the divergence of the equivalent currents the above equations can be augmented by the continuity equations

$$\nabla \cdot \mathbf{J}_H = -\partial_t \rho_H - \nabla P \cdot \mathbf{J} \quad \nabla \cdot \mathbf{J}_{mH} = -\partial_t \rho_{mH} \tag{12}$$

It is also important to note that sources $\mathbf{J}_{mH}$ and $\mathbf{J}_H$ are not independent. This can be seen, by adopting the approach used by [25],

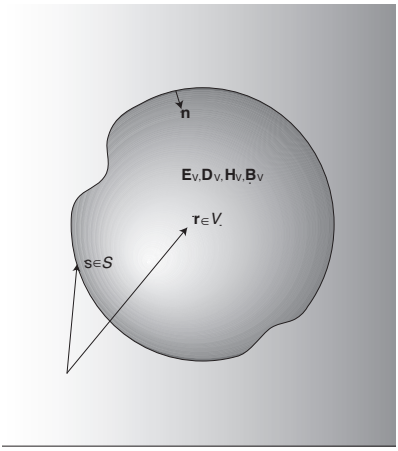

Figure 1. Volume V and its surface S having normal unit vector $\mathbf{n}$. Fields $\mathbf{E}_V$, $\mathbf{D}_V$, $\mathbf{H}_V$ and $\mathbf{B}_V$ are zero outside V.

as follows. It is assumed that the linear medium is isotropic with constitutive relations

$$\mathbf{D} = \epsilon \mathbf{E} \tag{13}$$

$$\mathbf{B} = \mu \mathbf{H} \tag{14}$$

where ϵ and μ are the (scalar) electrical permittivity and the magnetic permeability, respectively, and that all sources are outside V, i.e., $\mathbf{J}_V$, $\rho_V = 0$. Note that in geophysical situations considered in this paper volume V represents the region between the ionosphere and the ground, which is to a good approximation source-free. By using the simplifying assumptions, Eqs. (2) and (3) can be written for sources having temporal dependence of the form $e^{i\omega t}$ with angular frequency ω as

$$\nabla \times \mathbf{E}_V + i\omega\mu \mathbf{H}_V = -\mathbf{J}_{mH} \tag{15}$$

$$\nabla \times \mathbf{H}_V - i\omega\epsilon \mathbf{E}_V = \mathbf{J}_H \tag{16}$$

Then by substituting Eq. (15) into the curl of Eq. (16) separately for equivalent magnetic and electric sources, one obtains

$$\nabla \times (\nabla \times \mathbf{H}_V^e) - \omega^2 \mu\epsilon \mathbf{H}_V^e = \nabla \times \mathbf{J}_H \tag{17}$$

$$\nabla \times (\nabla \times \mathbf{H}_V^m) - \omega^2 \mu\epsilon \mathbf{H}_V^m = -i\omega\epsilon \mathbf{J}_{mH} \tag{18}$$

where superscripts e and m denote the fields generated by the electric and magnetic sources, respectively. By subtracting Eq. (18) from

Eq. (17) one then obtains

$$\nabla \times (\nabla \times (\mathbf{H}_V^e - \mathbf{H}_V^m)) - \omega^2 \mu\epsilon(\mathbf{H}_V^e - \mathbf{H}_V^m) = \nabla \times \mathbf{J}_H + i\omega\epsilon \mathbf{J}_{mH} \quad (19)$$

The equivalent form of the sources is then found by requiring that the field $(\mathbf{H}_V^e - \mathbf{H}_V^m)$ vanishes, i.e., $\mathbf{H}_V^e = \mathbf{H}_V^m$, which occurs for a *given* source when the source on the right-hand side of Eq. (19) is zero, i.e.,

$$\mathbf{J}_{mH} = -\frac{\nabla \times \mathbf{J}_H}{i\omega\epsilon} \quad (20)$$

Further, by using the equivalence (20), one can write Eqs. (15) and (16) as

$$\nabla \times \mathbf{E}_V + i\omega\mu\mathbf{H}_V = \frac{\nabla \times \mathbf{J}_H}{i\omega\epsilon} \quad (21)$$

$$\nabla \times \mathbf{H}_V - i\omega\epsilon\mathbf{E}_V = \mathbf{J}_H \quad (22)$$

which can be written by making a substitution $\mathbf{E}'_V = \mathbf{E}_V - \mathbf{J}_H/i\omega\epsilon$ as

$$\nabla \times \mathbf{E}'_V + i\omega\mu\mathbf{H}_V = 0 \quad (23)$$

$$\nabla \times \mathbf{H}_V - i\omega\epsilon\mathbf{E}'_V = 2\mathbf{J}_H \quad (24)$$

By comparing Eqs. (15) and (16) to Eqs. (23) and (24) it is seen that when fields in V and not on S are of interest, the equivalent magnetic source current can be replaced by doubling the equivalent electric current. Identical treatment, not repeated here, can be given to obtain a rule for replacing the equivalent electric source by a magnetic source.

Finally, by writing the rule for replacing the equivalent magnetic current by doubling the equivalent electric current as

$$(\mathbf{J}_H, \mathbf{J}_{mH}) \rightarrow (2\mathbf{J}_H, 0) \quad (25)$$

it can be seen from the continuity Eq. (12) that the replacement generates corresponding changes also for the equivalent charges. Namely

$$(\rho_H, \rho_{mH}) \rightarrow (2\rho_H, 0) \quad (26)$$

Thus, also the equivalent magnetic charge is replaced by doubling the electric charge.

2.2. Planar Equivalent Sources for a Vertical Line Current Element

Due to its common use in space weather applications (e.g., [14, 15, 17]), it is of interest to revisit the derivation of the equivalent sources for

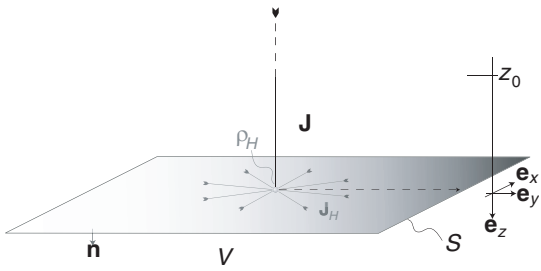

Figure 2. Vertical current element of length z_0 as a part of a divergence-free current system $\mathbf{J}_{tot}$ (dashed line). Transparent elements show the equivalent representation of the vertical current element $\mathbf{J}$ in terms of an equivalent electric current ($\mathbf{J}_H$) and a charge (ρ_H) on the surface S. Note that the charge ρ_H is a distribution rather than a point source. The sources $-\mathbf{J}$, $\mathbf{J}_H$ and ρ_H together are nonradiating below the surface S.

a vertical line current element. The source equivalence is considered both in terms of the incident and the total (incident and reflected) fields.

First, the source equivalence in terms of only the incident field is considered. The source $\mathbf{J}$ is written in Cartesian coordinate system $\mathbf{r} = x\mathbf{e}_x + y\mathbf{e}_y + z\mathbf{e}_z$ with the choice $\mathbf{n} = \mathbf{e}_z$ (see Fig. 2) as

$$\mathbf{J} = \delta(x)\delta(y)\left(\Theta(z - z_0) - \Theta(z)\right) I e^{i\omega t}\mathbf{e}_z \tag{27}$$

where Θ is the Heaviside step function, I the amplitude of the current, $|z_0|$ the length of the current element and a harmonic temporal dependence is assumed. It is important to note that the current element is understood as a part of a continuous current loop so that in quasi-static situations considered below there is no charge accumulation, i.e., $\nabla \cdot \mathbf{J}_{tot} = 0$.

By using Eqs. (8) and (10) and by applying the replacement rule of doubling of the electric sources discussed in Section 2.1, the equivalent sources associated with the current in Eq. (27) can be obtained by computing

$$\mathbf{J}_H(\mathbf{s}) = \frac{2}{\mu}\delta(\mathbf{s})\mathbf{n} \times \mathbf{B}(\mathbf{s}) \tag{28}$$

$$\rho_H(\mathbf{s}) = 2\epsilon\delta(\mathbf{s})\mathbf{n} \cdot \mathbf{E}(\mathbf{s}) \tag{29}$$

where the argument $\mathbf{s}$ is shown to emphasize that the fields are evaluated at the surface S. The magnetic flux density and the electric

field in Eqs. (28)–(29) are obtained from the vector potential $\mathbf{A}$ by operations

$$\mathbf{E} = -i\omega\left(1 + \frac{1}{k^2}\nabla\nabla\cdot\right)\mathbf{A} \tag{30}$$

$$\mathbf{B} = \nabla \times \mathbf{A} \tag{31}$$

Note that due to the condition $\nabla\cdot\mathbf{J}_{tot} = 0$, the divergence of the vector potential in Eq. (30) vanishes if the retardation of the field is neglected. The vector potential is obtained from the expression

$$\mathbf{A} = \frac{\mu}{4\pi}\int_V \frac{[\mathbf{J}(\mathbf{r}')]}{|\mathbf{s}-\mathbf{r}'|}dV' \tag{32}$$

In Eq. (32) square brackets indicate that the time is understood as retarded, and the distance function $|\mathbf{s}-\mathbf{r}'|$ is understood, also with complex arguments, as $\sqrt{(\mathbf{s}-\mathbf{r}')\cdot(\mathbf{s}-\mathbf{r}')}$. For complex arguments the branch of the distance function is chosen so that the integral in Eq. (32) converges.

Inserting the source in Eq. (27) into Eq. (32) results in the integral

$$\mathbf{A} = \frac{\mu}{4\pi}\int_V \frac{\left[\mathbf{J}(\mathbf{r}')\right]}{|\mathbf{s}-\mathbf{r}'|}dV' = \frac{\mu}{4\pi}\mathbf{e}_z I e^{i\omega t}\int_{z_0}^{0}\frac{e^{-\frac{i\omega}{c}\sqrt{r^2+z'^2}}}{\sqrt{r^2+z'^2}}dz' \tag{33}$$

where c is the speed of light and $r^2 = x^2+y^2$. Geophysical applications in mind, the exponential term in the right-hand side of Eq. (33) can be expanded as

$$e^{-\frac{i\omega}{c}\sqrt{r^2+z'^2}} = \sum_{n=0}^{\infty}\frac{1}{n!}\left(-\frac{i\omega}{c}\sqrt{r^2+z'^2}\right)^n \tag{34}$$

The term $\sqrt{r^2+z'^2}$ in Eqs. (33)–(34) is maximized at $z' = z_0$. Thus by assuming a condition $\left|\frac{\omega}{c}\sqrt{r^2+z_0^2}\right| \ll 1$, to be discussed more in depth below, it is reasonable to truncate the series in Eq. (34) to the first few terms. By including only the first term from the expansion, i.e., by neglecting the field retardation, Eq. (33) can be solved to give

$$\frac{\mu}{4\pi}\int_V \frac{[\mathbf{J}(\mathbf{r}')]}{|\mathbf{s}-\mathbf{r}'|}dV' \approx -\frac{\mu}{4\pi}I e^{i\omega t}\log\left(\frac{\sqrt{r^2+z_0^2}+z_0}{r}\right)\mathbf{e}_z \tag{35}$$

Finally, by using the expression (35) in Eqs. (28)–(31) and by moving

into circular cylindrical coordinates one obtains

$$\mathbf{J}_H(\mathbf{s}) \approx \frac{Ie^{i\omega t}}{2\pi} \frac{z_0}{r\sqrt{r^2+z_0^2}} \delta(z)\mathbf{e}_r \tag{36}$$

$$\rho_H(\mathbf{s}) \approx Ie^{i\omega t} \frac{i\omega\mu\epsilon}{2\pi} \log\left(\frac{\sqrt{r^2+z_0^2}+z_0}{r}\right)\delta(z) \tag{37}$$

where $\mathbf{e}_r$ is the radial unit vector.

In a typical geophysical setting of interest the highest frequencies are of the order of 1 Hz. On the other hand, the length of the field-aligned currents carrying the current between the ionosphere and the magnetosphere is of the order of $1R_e \approx 6400$ km. Also, one is interested in the fields near the line current element and thus r is at maximum of the order of 1000 km. Using these upper estimates, one obtains $\left|\frac{\omega}{c}\sqrt{r^2+z_0^2}\right|$ of the order of 0.1. It follows that the truncation of the expansion in Eq. (34) to the first term is reasonable, i.e., typical geophysical situations of our interest are quasi-static. Furthermore, it should be noted that taking the limit $z_0 \to -\infty$ for Eqs. (36)–(37) is not strictly valid if $\omega \neq 0$. By taking first the limit $\omega \to 0$, the charge in Eq. (37) vanishes, and then by taking the limit $z_0 \to -\infty$ the equivalent source current for the vertical line current element can be reduced to

$$\mathbf{J}_H(r) = -\frac{I}{2\pi r}\mathbf{e}_r \tag{38}$$

The electric current distribution in Eq. (38) was used by [17] as an equivalent source for a half-infinite vertical line current element. However, as shown above, the distribution in Eq. (38) is the sole equivalent source for a vertical line current element only in static situations; if $\omega \neq 0$ the equivalent charge also needs to be considered. Interestingly, the apparent difference between the equivalent sources derived above and the single source used by [17] disappears when the source equivalence is considered in terms of the total (incident and the reflected) instead of only the incident field. This will be shown next.

The usage of only the first term of the expansion (34) is equivalent to neglecting the displacement current term in Maxwell's equations, and without the displacement current, the current included in Maxwell's equations is divergence-free. It follows that the current across the boundaries is continuous, and thus at the air-ground boundary one can write by using Ohm's law

$$\mathbf{E}_1\sigma_1 \cdot \mathbf{n} = \mathbf{E}_2\sigma_2 \cdot \mathbf{n} \tag{39}$$

where subscripts 1 and 2 refer to the electric fields and the conductivities of the air and ground, respectively. Since the ratio between the conductivity of the air ($\sigma_1 \sim 10^{-14}$ S/m) and the conductivity of the ground ($\sigma_2 \sim 0.1 - 10^{-3}$ S/m) is always of the order of 10^{-10} or less, it follows from Eq. (39) that the vertical electric field in the ground at the air-surface boundary is always to a good approximation zero, i.e., $\mathbf{E}_2 \cdot \mathbf{n} = 0$. For $\epsilon \neq 0$ this naturally implies $\mathbf{D}_2 \cdot \mathbf{n} = 0$.

The condition $\mathbf{D}_2 \cdot \mathbf{n} = 0$ is met if there exists a surface charge ρ_s generating a vertical electric flux that annihilates the incident flux. Then, in the air, the vertical component of the incident flux is doubled by the field due to the surface charge, which can be solved by using the continuity condition of the normal component of the electric flux density across the surface, i.e.,

$$\rho_s = (0 - 2\mathbf{D}) \cdot \mathbf{n} = -2\mathbf{D} \cdot \mathbf{n} = -2\epsilon \mathbf{E} \cdot \mathbf{n} \tag{40}$$

It is seen from the charge densities included in Eqs. (29) and (40) that if the ground is located immediately below the surface S at which the equivalent sources are located, the horizontal component of the electric field associated with the two charge distributions vanishes. It follows that from the viewpoint of the magnetic field and the total horizontal electric field on the ground, only the equivalent current needs to be considered. Accordingly, the usage of the current distribution in Eq. (38) as a sole equivalent source for a half-infinite vertical line current element, as was done by [17], is justified.

3. THEORY AND GEOPHYSICAL APPLICATIONS OF THE COMPLEX IMAGE METHOD

In this section, CIM is derived from EIT for a simplified treatment of the electromagnetic induction in the ground. In contrast to the treatment by [20] who derived CIM from EIT for a homogeneous ground, both the classical and extended CIM approximations of EIT are presented for layered ground structures. Also a linear element-based approach to the application of CIM is introduced.

3.1. Derivation of the Complex Image Method for Layered Ground Structures from the Exact Image Theory

Following the classical CIM derivation for layered ground structures given by [16], it is assumed that the surface impedance Z_s giving the ratio of the horizontal electric and magnetic fields on the ground does not depend on the spatial wavenumbers of the fields. This is a valid

assumption if the second (and higher) order gradients of the fields vanish [26]. Generally, the comparisons between the exact and CIM-based results have shown that the fields are smooth enough for the approximation to hold to a good degree for various source current distributions (e.g., [16, 17, 22]).

For planar impedance surfaces described in terms of Z_s the image functions of the EIT take the form [24, p. 225]‡ (for EIT treatment of a dipole source over impedance surface, see [27])

$$f^{TE}(\zeta) = \delta(\zeta) - \frac{2}{p} e^{-\frac{\zeta}{p}} \Theta(\zeta) \tag{41}$$

$$f^{TM}(\zeta) = -\delta(\zeta) - 2pk^2 e^{pk^2\zeta} \Theta(\zeta) \tag{42}$$

$$f_0(\zeta) = -\frac{2}{p} \frac{Z_s^2}{Z_s^2 - \eta^2} \left(e^{pk^2\zeta} - e^{-\frac{\zeta}{p}} \right) \Theta(\zeta) \tag{43}$$

where $k = \omega\sqrt{\mu\epsilon}$, $\eta = \sqrt{\mu/\epsilon}$ and

$$p = \frac{Z_s}{i\omega\mu_0} \tag{44}$$

p as defined in Eq. (44) is identifiable as a complex skin depth. The image currents $\mathbf{J}_I$ are obtained from the source current $\mathbf{J}$ by using the image functions in operations [24, p. 213]

$$\mathbf{J}_I = \left(f^{TE} \bar{\bar{1}} + f_0 \mathbf{e}_z \mathbf{e}_z \cdot \left(\bar{\bar{1}} + \frac{1}{k^2} \nabla\nabla \right) \right) \cdot \mathbf{J}_c \tag{45}$$

where

$$\bar{\bar{1}}_\perp = \bar{\bar{1}} - \mathbf{e}_z \mathbf{e}_z \tag{46}$$

$$\mathbf{J}_c = \bar{\bar{C}} \cdot \mathbf{J}(\bar{\bar{C}} \cdot \mathbf{r}) \tag{47}$$

$$\bar{\bar{C}} = \bar{\bar{1}} - 2\mathbf{e}_z \mathbf{e}_z \tag{48}$$

and where operator $\mathbf{e}_z\mathbf{e}_z$ is a dyad carrying out the projection to $\mathbf{e}_z$ and $\bar{\bar{1}}$ is a unit dyadic. Note that in the selected form of the image current in Eq. (45), the image function f^{TM} is not used at all.

The vector potential associated with the reflected electromagnetic field at $z \leq 0$ can be obtained from

$$\mathbf{A}_r = \frac{\mu}{4\pi} \int_0^\infty \int_V \frac{[\mathbf{J}_I(\mathbf{r}', \zeta)]}{|\mathbf{r} - \mathbf{r}' - \zeta\mathbf{e}_z|} dV' d\zeta \tag{49}$$

‡ Note that the sign for the image function f_0 in Eq. (7.164) of [24] is incorrect and needs to be changed.

The electric and magnetic fields are obtained from Eq. (49) by the operations (30) and (31). Note that here the surface of the Earth is located at $z = 0$ and $\mathbf{e}_z$ points towards the ground, which is opposite to the direction chosen, for example, in [20, 24]. It follows that the sign of $\zeta\mathbf{e}_z$ in the distance term of Eq. (49) is opposite to the one seen typically in the EIT literature.

As discussed by [24, p. 225–226], situations may occur where the integral in Eq. (49) associated with some of the image functions in Eqs. (41)–(43) does not converge. However, since the integration over z' in Eq. (49) can be carried out in the complex plane, the branch of the integrand in Eq. (49) can be chosen so that the potential $\mathbf{A}_r$ remains finite.

As is seen from Eqs. (41)–(43), the exact image of the original source is distributed along the ζ-axis. To simplify the situation, it is assumed that in the geophysical setting of interest the fields are quasi-static, i.e., only the first term of the expansion (34) is used. The f^{TE} image (function) part of Eq. (49) can then be expressed as

$$\mathbf{A}_r^{TE} = \frac{\mu}{4\pi}\int_0^\infty \int_V \frac{\mathbf{J}_c(\mathbf{r}')f^{TE}}{|\mathbf{r}-\mathbf{r}'-\zeta\mathbf{e}_z|}dV'd\zeta \tag{50}$$

which can be expanded by using the Taylor series of the distance term as

$$\mathbf{A}_r^{TE} = \frac{\mu}{4\pi}\int_V \mathbf{J}_c(\mathbf{r}')\sum_{n=0}^{\infty}\frac{1}{n!}\frac{\partial^n}{\partial\zeta^n}\frac{1}{|\mathbf{r}-\mathbf{r}'-\zeta\mathbf{e}_z|}\int_0^\infty(\zeta-\zeta_0)^n f^{TE}d\zeta dV' \tag{51}$$

where the derivative operates only on the distance term and the derivatives are evaluated at $\zeta = \zeta_0$. The "trick" is then to find an optimal value for ζ_0 in Eq. (51). The optimal ζ_0 is looked for here by setting the first moment and thus the first order term of the expansion (51) to zero, i.e.,

$$\int_0^\infty(\zeta-\zeta_0)f^{TE}d\zeta = 0 \tag{52}$$

Provided that $\mathrm{Re}(p) > 0$, the condition (52) yields for f^{TE} in Eq. (41) $\zeta_0 = 2p$. The expansion (51) can then be written as

$$\mathbf{A}_r^{TE} = -\frac{\mu}{4\pi}\int_V \frac{\mathbf{J}_c(\mathbf{r}')}{|\mathbf{r}-\mathbf{r}'-2p\mathbf{e}_z|}dV' + \mathbf{R}_n \tag{53}$$

where $\mathbf{R}_n$ indicates the second and higher order terms of Eq. (51). The first term on the right-hand side of Eq. (53) can be obtained also by

setting $f^{TE} = -\delta(\zeta - 2p)$, which is the image corresponding to the classical CIM derived by [16]. Here the image is seen to result from a planar impedance surface and truncation of the series expansion of the field expressions given by EIT to the first order term.

By using $\zeta_0 = 2p$ and f^{TE} in Eq. (41), $\mathbf{R}_n$ in Eq. (53) can be solved for a point source of amplitude I located at $x' = y' = 0$ and $z' = -h$ to give at $x = y = z = 0$

$$\mathbf{R}_n = \frac{\mu}{4\pi} I \sum_{n=2}^{\infty} (-1)^n \frac{1}{|2p+h|} \left(\frac{p}{2p+h} \right)^n \left((-2)^n - 2e^{-2}\Gamma(n+1,-2) \right) \mathbf{e}_v \quad (54)$$

where $\mathbf{e}_v$ is unit vector giving the orientation of the point source, Γ is an incomplete gamma function and it is required that $\mathrm{Re}(p) > 0$ and $\mathrm{Im}(p) \neq 0$. From Eq. (54) it is clear that for $\mathbf{R}_n$ to be negligible, and for the CIM approximation to be valid for the specified source, it is required that $|p| \ll h$. Repetition of the above treatment for the image function f_0 in Eq. (43), provided that $\mathrm{Re}(p) > 0$ and $\mathrm{Re}(pk^2) < 0$, results in $\zeta_0 = p - \frac{1}{pk^2}$. Accordingly, the corresponding requirement for $\mathbf{R}_n$ to be negligible for the point source is $\left| p - \frac{1}{pk^2} \right| \ll h$.

In a typical geophysical setting the source is located in the ionosphere at the height of about 110 km and one is interested in periods of about 1–1000 seconds. Then by using the plane wave surface impedance derived for southern Finland by [21], one can estimate the magnitudes of $\left| p - \frac{1}{pk^2} \right|$ and $|p|$ and compare them to the height h of the source. For the relatively long periods associated with geophysical signals $\left| p - \frac{1}{pk^2} \right|$ is several orders of magnitude larger than 110 km. It thus follows, that the f_0 image cannot be approximated by means of the classical CIM. Furthermore, for the specified geophysical situation throughout the range of periods 1–1000 seconds the condition $\mathrm{Re}(pk^2) < 0$ is not fulfilled. Consequently, the integral in Eq. (52) does not converge for the f_0 image and the optimal ζ_0 cannot, in fact, be determined. However, with the settings above, $|p|$ varies from about 4 to 60 km from the shortest to the longest period. It follows that the classical CIM approximation for the f^{TE} image is, and crucially from the viewpoint of actual applications of the method, valid. Anyhow, it is quite clear that the approximation becomes poor also for the f^{TE} image at periods much longer than about 100 s. This was demonstrated for approximate EIT images derived by [20] by [28].

3.2. Derivation of an Extended Complex Image Method

It was seen above that the reflected electromagnetic field associated with the quasi-static volume current $\mathbf{J}$ can be expressed by means of vector potential

$$\mathbf{A}_r = \frac{\mu}{4\pi}\int_0^\infty \int_V \frac{\left(f^{TE}\bar{\bar{1}} + f_0 \mathbf{e}_z\mathbf{e}_z \cdot \left(\bar{\bar{1}} + \frac{1}{k^2}\nabla\nabla\right)\right)\cdot \mathbf{J}_c(\mathbf{r}')}{|\mathbf{r}-\mathbf{r}'-\zeta\mathbf{e}_z|} dV' d\zeta \quad (55)$$

It was also seen that the f^{TE} part of the expression (55) can be approximated as

$$\mathbf{A}_r^{TE} = -\frac{\mu}{4\pi}\int_V \frac{\mathbf{J}_c(\mathbf{r}')}{|\mathbf{r}-\mathbf{r}'-2p\mathbf{e}_z|} dV' \quad (56)$$

However, the fields associated with the f_0 image cannot be approximated by means of classical CIM. For a divergence-free current $\mathbf{J}$, also the reflected current $\mathbf{J}_c = \bar{\bar{C}}\cdot\mathbf{J}(\bar{\bar{C}}\cdot\mathbf{r}')$ is divergence-free and the field associated with the f_0 image in Eq. (55) simplifies to

$$\mathbf{A}_r^0 = \frac{\mu}{4\pi}\int_0^\infty \int_V \frac{(f_0\mathbf{e}_z\mathbf{e}_z)\cdot\mathbf{J}_c(\mathbf{r}')}{|\mathbf{r}-\mathbf{r}'-\zeta\mathbf{e}_z|} dV' d\zeta \quad (57)$$

If the divergence-free current $\mathbf{J}$ is perpendicular to $\mathbf{e}_z$, the term (57) vanishes and the reflected electromagnetic field is expressed solely by Eq. (56) and we obtain the classical CIM. However, if $\mathbf{J}$ is not perpendicular to $\mathbf{e}_z$ everywhere, the term (57) needs to be considered as well.

In principle, the non-CIM feature of the f_0 image can be avoided by mapping $\mathbf{J}$ into equivalent sources on plane S and thus by converting source currents to be perpendicular to $\mathbf{e}_z$. As was seen in Section 2.2, the equivalent mapping may also generate a charge distribution on S. However, it was shown that in geophysical situations the horizontal electric field generated by the equivalent charge distribution is annihilated by the surface charge required by the current continuity. It follows that if the magnetic field and the horizontal components of the electric field are of interest, one can neglect the equivalent charge and the fields can be computed by applying the classical CIM to the equivalent currents perpendicular to $\mathbf{e}_z$. This was the approach used by [17] who took into account also the fields generated by the vertical current elements. In more general situations, however, equivalent mapping would constitute an extra step that is not in fact necessary as will be shown below.

In typical geophysical situations such as the one considered in Section 3.1, it holds $\eta^2 \gg |Z_s^2|$ and $|1/p| \gg |pk^2|$. It follows that the

image function f_0 in Eq. (43) can be written to a good approximation as

$$f_0(\zeta) \approx -2pk^2 \left(1 - e^{-\frac{\zeta}{p}}\right) \Theta(\zeta) \tag{58}$$

Due to the condition $|1/p| \gg |pk^2|$ it is clear that the fields associated with the f_0 image are generally much weaker than those associated with the f^{TE} image. However, the factor $1/k^2$ in Eq. (30) cancels k^2 in Eq. (58) and thus the electric field associated with the divergence of the vector potential is not necessarily negligible. Also note that although the source current $\mathbf{J}$ is divergence-free, the divergence of the vector potential in Eq. (57) does not necessarily vanish as only the component parallel to $\mathbf{e}_z$ is considered.

By using Eqs. (30) and (57), the electric field associated with the divergence of the vector potential can be written as

$$\mathbf{E}_r^0 = -\frac{i\omega\mu}{4\pi k^2} \nabla \partial_z \int_0^\infty \int_V \frac{f_0(\mathbf{e}_z \cdot \mathbf{J}_c(\mathbf{r}'))}{|\mathbf{r} - \mathbf{r}' - \zeta \mathbf{e}_z|} dV' d\zeta \tag{59}$$

By using the identity

$$\partial_z \frac{1}{|\mathbf{r} - \mathbf{r}' - \zeta \mathbf{e}_z|} = -\partial_\zeta \frac{1}{|\mathbf{r} - \mathbf{r}' - \zeta \mathbf{e}_z|} \tag{60}$$

and partial integration over the coordinate ζ, one obtains

$$\mathbf{E}_r^0 = -\frac{i\omega\mu}{4\pi k^2} \nabla \int_0^\infty \int_V \frac{f_0'(\mathbf{e}_z \cdot \mathbf{J}_c(\mathbf{r}'))}{|\mathbf{r} - \mathbf{r}' - \zeta \mathbf{e}_z|} dV' d\zeta \tag{61}$$

By introducing the approximation (58) into Eq. (61) and by using the complex image approximation by means of truncating the expansion of the EIT expressions to the first order term and by using the condition in Eq. (52) for the approximate image function f_0' one obtains

$$\mathbf{E}_r^0 = \frac{i\omega\mu}{2\pi} p \nabla \int_V \frac{(\mathbf{e}_z \cdot \mathbf{J}_c(\mathbf{r}'))}{|\mathbf{r} - \mathbf{r}' - p\mathbf{e}_z|} dV' \tag{62}$$

Eq. (62) is of the form $\mathbf{E}_r^0 = -\nabla\Phi$ where Φ is the quasi-electrostatic potential depending on charge distributed as a function of $(\mathbf{e}_z \cdot \mathbf{J}_c(\mathbf{r}'))$. It can thus be interpreted that in contrast to image currents associated with the f^{TE} image, the electric field $\mathbf{E}_r^0$ is associated with (complex) image charge. Note that in the case of an image charge, the source is shifted by p instead of $2p$ in the direction of the z-axis.

It is of interest to see how Eq. (62) compares to the horizontal electric field associated with half-infinite line current element derived

by [17]. The fields are evaluated on the ground. For this, one inserts the source in Eq. (27) into Eq. (62) and takes the limit $z_0 \to -\infty$ to obtain for $z = -h$ following expression for the horizontal electric field

$$\mathbf{E}^0_{r\perp} = \frac{i\omega\mu}{2\pi} I e^{i\omega t} p \left(\frac{r}{\sqrt{r^2+(h+p)^2}\left(h+p+\sqrt{r^2+(h+p)^2}\right)} \right) \mathbf{e}_r \quad (63)$$

As the incident electric field and the field associated with the f^{TE} image do not have horizontal component for the studied setup, the expression (63) is the total horizontal electric field associated with a half-infinite vertical source current. The corresponding total field derived by [17] is

$$\mathbf{E}^0_{r\perp} = \frac{i\omega\mu}{4\pi} I e^{i\omega t} \left(\frac{r}{h+\sqrt{r^2+h^2}} - \frac{r}{h+2p+\sqrt{r^2+(h+2p)^2}} \right) \mathbf{e}_r \quad (64)$$

It is seen by comparing Eqs. (63) and (64) that the fields obtained by the two approaches are not identical. However, in geophysical settings of interest the difference is negligible as is seen from Fig. 3 where

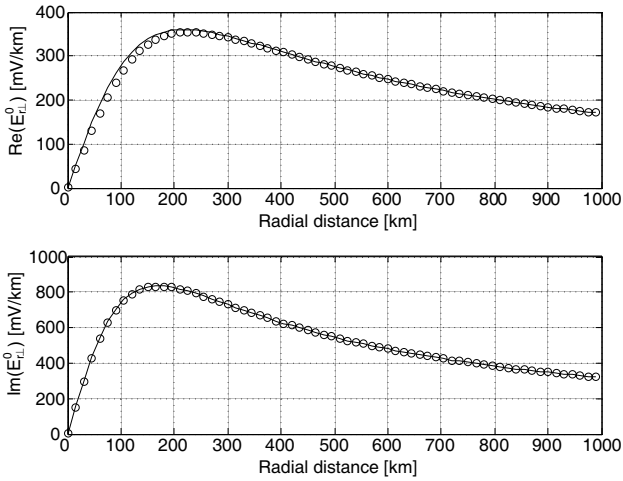

Figure 3. Top panel: the real part of the radial horizontal electric field given by Eqs. (63) (circles) and (64). Bottom panel: the imaginary part of the radial horizontal electric field given by Eqs. (63) (circles) and (64). The fields were evaluated on the ground by using the period of 100 s, $I = 10^6$ A, $h = 110$ km, the vacuum permeability and the plane wave surface impedance derived for southern Finland by [21].

the fields were evaluated by using the period of 100 s, $I = 10^6$ A, $h = 110$ km, the vacuum permeability and the plane wave surface impedance derived for southern Finland by [21].

Summarizing, it was shown that the electric field associated with the f_0 image, which cannot be approximated directly by means of the classical CIM, can be expressed in a simplified form for a quasi-static divergence-free source current $\mathbf{J}$. The derived electric field expression (62) associated with an image charge can be considered as an extension to the classical CIM. Further, in the limiting case of a vertical half-infinite source current the extension was seen to be (to a good approximation) equivalent with the CIM extension by [17].

3.3. Generalized Application of the Extended CIM

The following approach will be used to generalize the CIM-based computation of the electromagnetic fields generated by quasi-static divergence-free volume currents. The source current $\mathbf{J}$ is expressed as a linear superimposition of N linear elements (see Fig. 4). Formally,

$$\mathbf{J}(\mathbf{r}) = \sum_{i=1}^{N} \mathbf{J}_i \tag{65}$$

Due to the linearity of Maxwell's equations, the total (incident and reflected) electromagnetic field associated with the elements can be expressed as

$$\mathbf{E}(\mathbf{r}) = \sum_{i=1}^{N} \mathbf{E}_i \quad \mathbf{B}(\mathbf{r}) = \sum_{i=1}^{N} \mathbf{B}_i \tag{66}$$

where $\mathbf{E}_i$ and $\mathbf{B}_i$ are the fields generated by an element $\mathbf{J}_i$. The fields associated with individual elements are obtained by the following procedure. First, one computes the electromagnetic field generated by an element $\mathbf{J}'_{el}$ of length Δl in the coordinates $\mathbf{r}'$ (see Fig. 4)

$$\mathbf{J}'_{el}(\mathbf{r}') = \delta(x')\delta(z')\Theta(y')\Theta(\Delta l - y')Ie^{i\omega t}\mathbf{e}_{y'} \tag{67}$$

It can be shown that the source (67) gives rise to an incident electromagnetic field

$$\mathbf{E}'_{el}(\mathbf{r}') = \frac{i\omega\mu}{4\pi} Ie^{i\omega t} \log\left(\frac{-y' + \sqrt{r_1^2 + z'^2}}{-y' + \Delta l + \sqrt{r_2^2 + z'^2}}\right)\mathbf{e}_{y'} \tag{68}$$

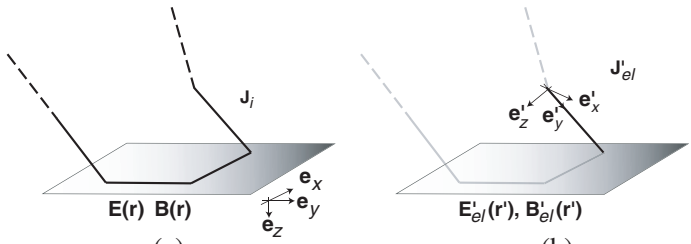

Figure 4. Panel (a) quasi-static divergence-free source current system $\mathbf{J}(\mathbf{r})$ presented as a superimposition of linear current elements. Panel (b) a single element $\mathbf{J}_i$ of the current system and the electromagnetic field associated with the element in the coordinates $\mathbf{r}' = \bar{\bar{R}}_i \cdot (\mathbf{r} - \Delta\mathbf{r}_i)$ were operator $\bar{\bar{R}}_i$ carries out the rotation of the coordinate system and $\Delta\mathbf{r}_i$ the translation of the origin.

$$\mathbf{B}'_{el}(\mathbf{r}') = \frac{\mu}{4\pi} I e^{i\omega t} \left(\frac{1}{\sqrt{r_2^2 + z'^2}\left(-y' + \Delta l + \sqrt{r_2^2 + z'^2}\right)} - \frac{1}{\sqrt{r_1^2 + z'^2}\left(-y' + \sqrt{r_1^2 + z'^2}\right)} \right) \left(x'\mathbf{e}_{z'} - z'\mathbf{e}_{x'}\right) \quad (69)$$

where r_1^2 and r_2^2 denote $x'^2 + y'^2$ and $x'^2 + (y' - \Delta l)^2$, respectively. The electric field associated with the f_0 image is in turn obtained by substituting the source (67) into Eq. (62). In using Eq. (62), one computes the field associated with the non-reflected and non-translated source, i.e.,

$$\mathbf{E}'^0_{r,el} = \frac{i\omega\mu}{2\pi} p \nabla' \int_V \frac{(\mathbf{e}_z \cdot \mathbf{J}'_{el}(\mathbf{r}''))}{|\mathbf{r}' - \mathbf{r}''|} dV'' \quad (70)$$

which gives

$$\mathbf{E}'^0_{r,el} = \frac{i\omega\mu}{2\pi} p I e^{i\omega t} \sin(\vartheta) \left[\left(\frac{1}{\sqrt{r_1^2 + z'^2}\left(y' + \sqrt{r_1^2 + z'^2}\right)} - \frac{1}{\sqrt{r_2^2 + z'^2}\left(y' - \Delta l + \sqrt{r_2^2 + z'^2}\right)} \right) \left(x'\mathbf{e}_{x'} + z'\mathbf{e}_{z'}\right) + \left(\frac{1}{\sqrt{r_1^2 + z'^2}} - \frac{1}{\sqrt{r_2^2 + z'^2}} \right) \mathbf{e}_{y'} \right] \quad (71)$$

where the angle ϑ is obtained from Eq. (75).

The total electromagnetic field generated by an element is obtained by a superimposition of the incident field, the reflected field associated with the approximate f^{TE} image and the reflected electric field associated with the approximate f_0 image. Accordingly, the total field associated with an element $\mathbf{J}_i$ is obtained in the coordinates $\mathbf{r}$ from Eqs. (68), (69) and (71) by computing

$$\begin{aligned}\mathbf{E}_i(\mathbf{r}) \;=\; & \bar{\bar{R}}_i^{-1} \cdot \mathbf{E}'_{el}(\bar{\bar{R}}_i \cdot (\mathbf{r} - \Delta\mathbf{r}_i)) \\ & -\bar{\bar{R}}_{ci}^{-1} \cdot \mathbf{E}'_{el}(\bar{\bar{R}}_{ci} \cdot (\mathbf{r} - \bar{\bar{C}} \cdot \Delta\mathbf{r}_i - 2p\mathbf{e}_z)) \\ & +\bar{\bar{R}}_{ci}^{-1} \cdot \mathbf{E}'^{0}_{r,el}(\bar{\bar{R}}_{ci} \cdot (\mathbf{r} - \bar{\bar{C}} \cdot \Delta\mathbf{r}_i - p\mathbf{e}_z)) \qquad (72) \\ \mathbf{B}_i(\mathbf{r}) \;=\; & \bar{\bar{R}}_i^{-1} \cdot \mathbf{B}'_{el}(\bar{\bar{R}}_i \cdot (\mathbf{r} - \Delta\mathbf{r}_i)) \\ & -\bar{\bar{R}}_{ci}^{-1} \cdot \mathbf{B}'_{el}(\bar{\bar{R}}_{ci} \cdot (\mathbf{r} - \bar{\bar{C}} \cdot \Delta\mathbf{r}_i - 2p\mathbf{e}_z)) \qquad (73)\end{aligned}$$

where operators $\bar{\bar{R}}_i$ and $\bar{\bar{R}}_{ci}$ carry out the rotation of the coordinates needed to obtain different orientations of the source currents (and the electromagnetic field), and $\Delta\mathbf{r}_i$ is the translation of the origin of the coordinate system used to obtain different locations of the sources. The derivation of the transformations used in the expressions (72) and (73) is given in Appendix A.

For example, if the two end-points of the element are (x_1, y_1, z_1) and (x_2, y_2, z_2), the angles φ and ϑ associated with $\bar{\bar{R}}_i$ (and $\bar{\bar{R}}_{ci}$) that transforms the element to be aligned with the y'-axis, as was chosen in Eq. (67), are obtained by computing

$$\varphi \;=\; \tan^{-1}\left(\frac{y_0}{x_0}\right) - \frac{\pi}{2} \qquad (74)$$

$$\vartheta \;=\; \cos^{-1}\left(\frac{z_0}{\sqrt{x_0^2 + y_0^2 + z_0^2}}\right) - \frac{\pi}{2} \qquad (75)$$

where now $x_0 = x_2 - x_1$, $y_0 = y_2 - y_1$, $z_0 = z_2 - z_1$. The translation is $\Delta\mathbf{r} = (x_1, y_1, z_1)$. The total electromagnetic field generated by the source $\mathbf{J}$ in Eq. (65) is obtained by superimposing the fields generated by the individual elements as indicated by Eq. (66).

The generalized application of the extended CIM was verified by means of the following example. The external current system of the setup was composed of a horizontal current segment at height 110 km and flowing from the origin of the (x, y)-plane to the distance of 200 km along the positive y-axis. Both ends of the horizontal segment are coupled to linear segments in (x, z)-plane having 45 degree angle with

respect to the horizontal plane. The current loop having amplitude of $I = 10^6$ A is closed in the infinity. Again, layered ground model derived for southern Finland by [21] was used in the calculations. The total electromagnetic field generated by the external current system was computed on the ground at $z = 0$ for the period of 100 s using both the extended CIM as described above and the exact formulation by [18].

The results of the verification calculations are given in Figs. 5 and 6 where the imaginary and the real parts of the total electric and magnetic field are shown, respectively. The results for the real and imaginary parts of the electric and magnetic field, respectively, are similar (not shown). It is seen that the fields computed by means of extended CIM and the exact formulation by [18] are practically

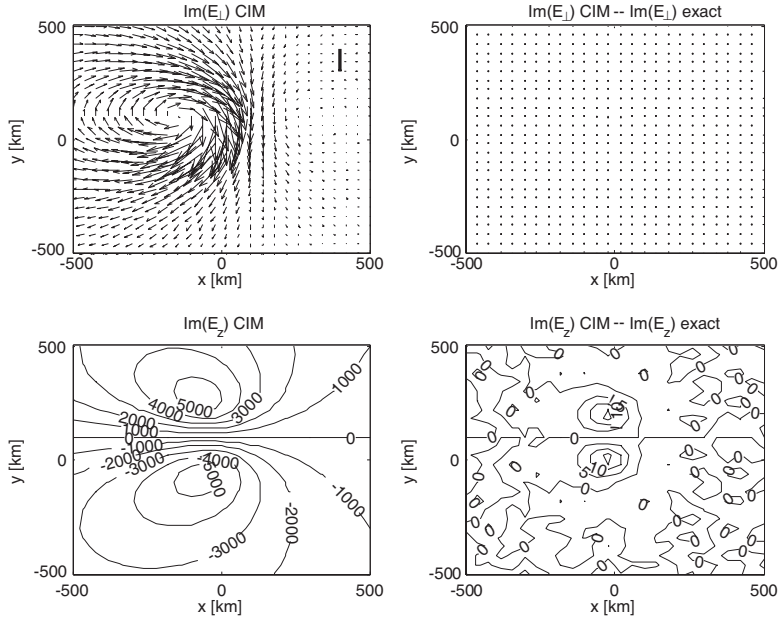

Figure 5. The imaginary parts of the total horizontal (top left) and the vertical (bottom left) electric field computed by means of extended CIM and the difference between the fields obtained by extended CIM and the exact formulation by [18] (right column). See the text for the setup of the computations. The scale for the top row is indicated in the top right corner of the first panel, which shows vector length corresponding to the electric field amplitude of 1000 mV/km. The unit in the bottom row is mV/km.

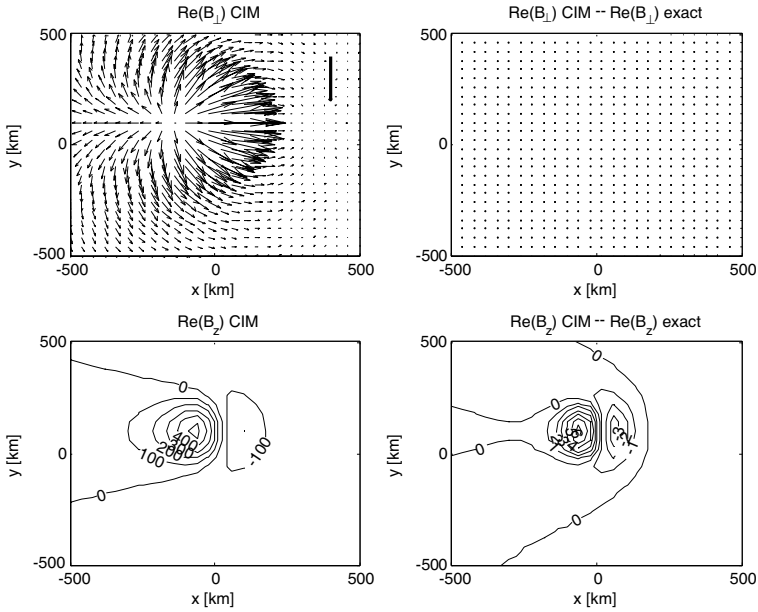

Figure 6. The real parts of the total horizontal (top left) and the vertical (bottom left) magnetic field computed by means of extended CIM and the difference between the fields obtained by extended CIM and the exact formulation by [18] (right column). See the text for the setup of the computations. The scale for the top row is indicated in the top right corner of the first panel, which shows vector length corresponding to the magnetic field amplitude of 1000 nT. The unit in the bottom row is nT.

identical. Consequently, it can be concluded that for the given setup the extended CIM provides a very accurate approximation for the electromagnetic fields.

4. SUMMARY

In this work, source equivalence and computation of the reflected (induced) electromagnetic field in geophysical situations were studied. It was shown that the application of Huygens' principle [23] allows for full generalization of Fukushima's equivalence theorem [19] that applies only to the magnetic field. The source equivalence was revisited for a vertical line current element, and it was shown that the equivalent charge required to replace the original source by a planar equivalent source together with the surface charge associated with the reflected

field generates a purely vertical total electric field on the ground. This explains why the CIM application introduced by [17] works for both the magnetic field and horizontal components of the electric field although only equivalent currents are considered.

The classical CIM was derived from EIT for planar impedance surfaces, condition which requires that the second (and higher) order gradients of the fields on the ground vanish. The classical CIM was seen to result from truncation of the series expansion of the EIT expressions to the first order term. Then the classical CIM was extended by considering a divergence-free source current that may have components also perpendicular to the ground plane. The extension that was seen to generate a complex image charge is not present in the classical CIM. Importantly, the electric field associated with the image charge was seen to merge in the limiting case of a vertical half-infinite source current with the CIM extension by [17].

A generalized application of the extended CIM to geophysical situations having divergence-free volume source currents was introduced. The application involves decomposition of the source into linear current elements and rotations, translations and reflections of the electromagnetic field expressions associated with each element. Expressions needed for rotations, translations and reflections that result from general transformation rules for Maxwell's equations were also provided. The generalized element representation combined with the derived extended CIM expressions will allow a computationally efficient consideration of the electromagnetic induction in a layered ground in situations where the source currents have arbitrary orientations with respect to the ground plane. The validity of the new approach was verified for an example external current system and ground model setup by means of comparisons to results obtained from exact formulation by [18].

In summary, this study provided the following new contributions. 1) It was rigorously proofed that CIM by [17] is valid although only equivalent currents are considered. 2) CIM was extended to situations where the source current can have any orientation. The method in [17] is restricted to high geomagnetic latitudes, but the general approach enables treatment of geomagnetic induction problems at all latitudes. 3) A practical CIM application technique was derived based on a current element representation and coordinate transformations carried out in the complex space. The validity of the new results was demonstrated by using an independent analytical model of three-dimensional ionospheric currents.

ACKNOWLEDGMENT

We gratefully acknowledge Prof. Ismo Lindell for his valuable comments on the paper.

APPENDIX A. ROTATION, REFLECTION AND TRANSLATION OF THE SOURCE CURRENT

To express the effect of rotations, reflections and translations of the source current on the corresponding electromagnetic field, one needs transformation rules for Maxwell's equations. This in mind, it can be shown that a transformation from a system of equations in Cartesian coordinates $\mathbf{r}$ to another coordinate system carried out by mapping $\mathbf{r}' = \mathbf{g}(\mathbf{r})$ results in another "Cartesian" form of the equations (e.g., [25, 26, p. 144–159]) (see also [27, and references therein]). The invariance requires that the fields, constitutive parameters and the sources are transformed as

$$\mathbf{E}' = \left(\bar{\bar{J}}^T\right)^{-1} \cdot \mathbf{E} \tag{A1}$$

$$\mathbf{H}' = \left(\bar{\bar{J}}^T\right)^{-1} \cdot \mathbf{H} \tag{A2}$$

$$\bar{\bar{\epsilon}}' = \frac{\bar{\bar{J}} \cdot \bar{\bar{\epsilon}} \cdot \bar{\bar{J}}^T}{\det\left(\bar{\bar{J}}\right)} \tag{A3}$$

$$\bar{\bar{\mu}}' = \frac{\bar{\bar{J}} \cdot \bar{\bar{\mu}} \cdot \bar{\bar{J}}^T}{\det\left(\bar{\bar{J}}\right)} \tag{A4}$$

$$\mathbf{J}' = \frac{\bar{\bar{J}} \cdot \mathbf{J}}{\det\left(\bar{\bar{J}}\right)} \tag{A5}$$

$$\rho' = \frac{\rho}{\det\left(\bar{\bar{J}}\right)} \tag{A6}$$

where $\bar{\bar{J}}$ is the Jacobian of the transformation $\mathbf{r} \rightarrow \mathbf{r}'$ and $\bar{\bar{\epsilon}}$ and $\bar{\bar{\mu}}$ are the permittivity and permeability tensors, respectively.

A combined rotation and translation of the coordinates can be defined as a transformation

$$\mathbf{r}' = \bar{\bar{R}} \cdot (\mathbf{r} - \Delta\mathbf{r}) \tag{A7}$$

where the operator $\bar{\bar{R}}$ is defined as

$$\bar{\bar{R}} = \begin{pmatrix} \cos(\varphi) & \sin(\varphi) & 0 \\ -\cos(\vartheta)\sin(\varphi) & \cos(\vartheta)\cos(\varphi) & -\sin(\vartheta) \\ -\sin(\vartheta)\sin(\varphi) & \sin(\vartheta)\cos(\varphi) & \cos(\vartheta) \end{pmatrix} \tag{A8}$$

In Eq. (A8) the rotation φ is made counter-clockwise keeping the z-axis constant and rotation ϑ is made clockwise keeping the rotated x-axis constant. For the transformation (A7) it holds

$$\bar{\bar{J}} = \bar{\bar{R}} \qquad \det\left(\bar{\bar{R}}\right) = 1 \qquad \bar{\bar{R}}^T = \bar{\bar{R}}^{-1} \tag{A9}$$

By writing the reflection operator $\bar{\bar{C}}$ as

$$\bar{\bar{C}} = \bar{\bar{1}} - 2\mathbf{nn} = \begin{pmatrix} 1 & 0 & 0 \\ 0 & 1 & 0 \\ 0 & 0 & -1 \end{pmatrix} \tag{A10}$$

where the normal unit vector $\mathbf{n}$ is assigned to the third component of a vector (i.e., $\mathbf{n} = \mathbf{e}_z$), the combined reflection with respect to $\mathbf{e}_z$, rotation and translation can be carried out by the transformation

$$\mathbf{r}' = \bar{\bar{R}}_c \cdot (\mathbf{r} - \bar{\bar{C}} \cdot \Delta\mathbf{r}) \tag{A11}$$

where the operator $\bar{\bar{R}}_c$ is obtained from Eq. (A8) by substitution $\vartheta = -\vartheta$. The transformation (A11) fulfills identities identical to those in Eq. (A9).

The effect of the rotation and translation of the source on the electromagnetic field can be seen from Eqs. (A1), (A2), (A5). Namely, if the source is translated and rotated as

$$\mathbf{J}'(\mathbf{r}') = \bar{\bar{R}} \cdot \mathbf{J} \tag{A12}$$

where $\mathbf{r}'$ is given by Eq. (A7), the fields in coordinate system $\mathbf{r}$ can be obtained from

$$\mathbf{E}(\mathbf{r}) = \bar{\bar{R}}^{-1} \cdot \mathbf{E}' \tag{A13}$$

$$\mathbf{H}(\mathbf{r}) = \bar{\bar{R}}^{-1} \cdot \mathbf{H}' \tag{A14}$$

For a medium linear and isotropic in the coordinates $\mathbf{r}$, by using Eqs. (14) and (A4), Eq. (A14) can be written for the magnetic flux density as

$$\mathbf{B}(\mathbf{r}) = \bar{\bar{R}}^{-1} \cdot \mathbf{B}' \tag{A15}$$

Clearly, identical relations hold also for the fields associated with a source that is translated, rotated and reflected by means of the transformation (A11).

REFERENCES

1. Thomson, W., *Reprint of Papers on Electrostatics and Magnetism*, Macmillan & Co., 2nd Edition, 1884.
2. Taraldsen, G., "The complex image method," *Wave Motion*, Vol. 43, 91–97, 2005.
3. Wait, J. R., "Image theory of a quasi-static magnetic dipole over a dissipative half-space," *Electronics Letters*, Vol. 5, 281–282, 1969.
4. Wait, J. R. and K. P. Spies, "On the image representation of the quasistatic fields of a line current source above the ground," *Can. J. Phys.*, Vol. 47, 2731–2733, 1969.
5. Wait, J. R., "Complex image theory-revisited," *IEEE Antennas Propagat. Mag.*, Vol. 33, No. 4, 27–29, 1991.
6. Lindell, I. V. and E. Alanen, "Exact image theory for the Sommerfeld half-space problem, Part 1: Vertical magnetic dipole," *IEEE Transactions on Antennas and Propagation*, Vol. 32, 126–133, 1984.
7. Lindell, I. V. and E. Alanen, "Exact image theory for the Sommerfeld half-space problem, Part 2: Vertical electric dipole," *IEEE Transactions on Antennas and Propagation*, Vol. 32, 841–847, 1984.
8. Lindell, I. V. and E. Alanen, "Exact image theory for the Sommerfeld half-space problem, Part 3: General formulation," *IEEE Transactions on Antennas and Propagation*, Vol. 32, 1027–1032, 1984.
9. Deschamps, G. A., "Gaussian beam as a bundle of complex rays," *Electronics Letters*, Vol. 7, No. 23, 684–685, 1971.
10. Madden, T. M. and R. L. Mackie, "Three-dimensional magnetotelluric modelling and inversion," *Proceedings of the IEEE*, Vol. 77, No. 2, 318–333, 1989.
11. Avdeev, D. B., A. V. Kuvshinov, O. V. Pankratov, and O. G. Newman, "Three-dimensional induction logging problems, Part I: An integral equation solution and model comparisons," *Geophysics*, Vol. 67, No. 2, 413–426, 2002.
12. Silva-Macêdo, J. A., M. A. Romero, and B.-H. V. Borges, "An extended fdtd method for the analysis of electromagnetic field rotators and cloaking devices," *Progress In Electromagnetics Research*, PIER 87, 183–196, 2008.
13. Soleimani, M., "Simultaneous reconstruction of permeability and conductivity in magnetic induction tomography," *Journal of Electromagnetic Waves and Applications*, Vol. 23, No. 5/6, 785–

798, 2009.

14. Viljanen, A., O. Amm, and R. Pirjola, "Modeling geomagnetically induced currents during different ionospheric situations," *J. Geophys. Res.*, Vol. 104, No. A12, 28059–28072, 10.1029/1999JA900337, 1999.
15. Pulkkinen, A., M. Hesse, M. Kuznetsova, and L. Rastätter, "First-principles modeling of geomagnetically induced electromagnetic fields and currents from upstream solar wind to the surface of the Earth," *Annales Geophysicae*, Vol. 25, 881–893, 2007.
16. Thomson, D. J. and J. T. Weaver, "The complex image approximation for induction in a multilayered Earth," *J. Geophys. Res.*, Vol. 80, 123–129, 1975.
17. Pirjola, R. and A. Viljanen, "Complex image method for calculating electric and magnetic fields produced by an auroral electrojet of finite length," *Annales Geophysicae*, Vol. 16, 1434–1444, 1998.
18. Häkkinen, L. and R. Pirjola, "Calculation of electric and magnetic fields due to an electrojet current system above a layered earth," *Geophysica*, Vol. 22, No. 1–2, 31–44, 1986.
19. Fukushima, N., "Generalized theorem for no ground magnetic effect of vertical currents connected with Pedersen currents in the uniform conductivity ionosphere," *Rep. Ionos. Space Res. Jpn.*, Vol. 30, 35–40, 1976.
20. Lindell, I. V., J. J. Hänninen, and R. Pirjola, "Wait's complex-image principle generalized to arbitrary sources," *IEEE Transactions on Antennas and Propagation*, Vol. 48, 1618–1624, 2000.
21. Pulkkinen, A., R. Pirjola, and A. Viljanen, "Determination of ground conductivity and system parameters for optimal modeling of geomagnetically induced current flow in technological systems," *Earth, Planets and Space*, Vol. 99, 999–1006, 2007.
22. Boteler, D. H. and R. J. Pirjola, "The complex-image method for calculating the magnetic and electric fields produced at the surface of the Earth by the auroral electrojet," *Geophys. J. Int.*, Vol. 132, No. 1, 31–40, 1998.
23. Lindell, I., "Huygens' principle in electromagnetics," *IEE Proc.-Sci. Meas. Technol.*, Vol. 143, No. 2, 103–105, 1996.
24. Lindell, I., *Methods for Electromagnetic Field Analysis*, Oxford University Press, 1995.
25. Mayes, P. E., "The equivalence of electric and magnetic sources," *IRE Transactions on Ant. Propag.*, Vol. 6, 295–296, 1958.

26. Dmitriev, V. I. and M. N. Berdichevsky, "The fundamental model of magnetotelluric sounding," *Proc. IEEE*, Vol. 67, 1034–1044, 1979.
27. Sarabandi, K., M. D. Casciato, and Il-Sueh Koh, "Efficient calculation of the fields of a dipole radiating above an impedance plane," *IEEE Transactions on Antennas and Propagation*, Vol. 50, No. 9, 1222–1235, 2002.
28. Hänninen, J. J., R. J. Pirjola, and I. V. Lindell, "Application of the exact image theory to studies of ground effects of space weather," *Geophys. J. Int.*, Vol. 151, 534–542, 2002.
29. Ward, A. J. and J. B. Pendry, "Refraction and geometry in Maxwell's equations," *Journal of Modern Optics*, Vol. 43, 773–793, 1996.
30. Post, E. J., *Formal Structure of Electromagnetics, General Covariance and Electromagnetics*, Interscience Publishers, 1962.
31. Kosmas, L. T. and O. Hess, "Optics: Watch your back," *Nature*, Vol. 451, 27, 2008.